Adsorption and Desorption Equilibria of Nitrogen, Methane, Ethane, and Ethylene on Date-Pit Activated Carbon

Shaheen A. Al-Muhtaseb*

Department of Chemical Engineering, Qatar University, P.O. Box 2713, Doha, Qatar

Date pits were used to produce a highly porous activated carbon. The resulting date-pit activated carbon was used in a volumetric adsorption apparatus to measure the vapor-phase adsorption and desorption of nitrogen, methane, ethane, and ethylene over a wide range of pressure and at temperatures of (30, 45, and 60) °C. Being characterized with a relatively high surface area, the synthesized date-pit activated carbon exhibited a satisfactory capacity for adsorbing the various tested gases. However, the desorption of these gases exhibited a hysteresis phenomenon, especially at low temperatures. A Langmuir type model was proposed for fitting both the adsorption and the desorption data with hysteresis, and the corresponding isosteric heats of adsorption and desorption were estimated and compared.

1. Introduction

Separation processes are among the most important elements of the chemical, petroleum refining, and petrochemical industries. Vapor phase adsorption has received remarkable attention in the last few decades as a one of the most important separation processes.[1] This attention was due to new advances and developments of adsorbents that fit various industries. Because of the worldwide increasing demand and cost of energy sources, adsorption processes are becoming strong competitors for conventional separation processes in the chemical and petrochemical industries.[2] In fact, vapor-phase adsorption processes surpassed distillation processes in separating mixtures with high throughputs or close volatilities. Moreover, vapor-phase adsorption processes are known to result in highly pure products,[2] which classify them as purification processes. Therefore, separation processes can be revolutionized when implementing optimal adsorption processes. However, the proper modeling of adsorption processes depends on the availability of adsorption equilibrium data for these mixtures.[3] Nonetheless, since the adsorption phenomenon has the additional degree of freedom that is related to choice of the adsorbent, whenever the adsorbent is changed, all of the adsorption behavior data will change accordingly. Therefore, optimal adsorption processes cannot be designed without obtaining basic experimental adsorption data for such hydrocarbons on the selected adsorbents.

Activated carbons were prepared from locally available, agricultural byproduct, date pits that have shown a remarkable ability for the adsorption of species from liquid solutions.[4−9] Nonetheless, to the author's knowledge, there is no published work which addresses the use of date-pit activated carbons for vapor-phase adsorption. Therefore, this study will focus on using activated carbon prepared from date pits as a local adsorbent for the adsorption of nitrogen, methane, ethane, and ethylene over a wide range of pressure and at temperatures of (30, 45, and 60) °C. Such gas components are of high relevance to the natural gas and petrochemical industries.

* Corresponding author. Fax: +974 485-2491. Tel.: +974 485-2193. E-mail: s.almuhtaseb@qu.edu.qa.

Adsorption hysteresis arises when the adsorption and desorption curves do not coincide. This phenomenon is known to be exhibited for adsorbents which include mesopore structures. Specifically, it occurs for adsorbents which include pores with diameters above 4 nm.[10] Only very limited studies in the literature address the modeling of adsorption−desorption data with hysteresis. Overall, it was found that proper modeling of hysteresis requires very extensive considerations which include adopting complicated approaches such as density functional theory[11] and Monte Carlo simulations.[12−16] Recently, a model of cluster formation on functional groups was proposed,[17] which could successfully describe adsorption−desorption data with hysteresis. However, this model requires knowledge of adsorption clusters around functional groups within the adsorbent. Overall, to the author's knowledge, there are virtually no simple models available in the literature for fitting adsorption−desorption equilibrium data with hysteresis. Such simple models (e.g., Langmuir type isotherm models) would be very beneficial for understanding such behavior and the corresponding thermophysical properties that can be estimated from such models. These models also become handy for the simulation of adsorption−desorption processes under variable conditions.

In this work, a volumetric adsorption apparatus, which was designed and built in the UAE University laboratories,[18] was used to measure the adsorption equilibria of various gas compounds on activated carbon produced from date pits as an indigenous adsorbent material. The produced activated carbon was used to measure the adsorption and desorption isotherms of nitrogen, methane, ethane, and ethylene. Those hydrocarbon species were selected to be useful for simulating the separation of volatile organic compounds from gas mixtures. The measured data were correlated to a Langmuir type isotherm model, which takes into consideration the hysteresis effect. Furthermore, the corresponding isosteric heats of adsorption and desorption were estimated and compared.

2. Materials and Methods

Dried date pits were grinded and screened. The resulting date pit granules, contained between mesh size 200 and the pan, were collected to be carbonized and activated. These date pit granules

10.1021/je900350k CCC: $40.75
Published on Web 10/16/2009

Table 1. Measured Equilibrium Amount Adsorbed (n) of Nitrogen on Date-Pit Activated Carbon versus Increasing Pressure (P) from T = (30 to 60) °C

P atm	n mol·kg^{-1}	P atm	n mol·kg^{-1}	P atm	n mol·kg^{-1}
		T = 30 °C			
0.365	0.059	1.918	0.343	4.605	0.613
0.632	0.113	2.531	0.423	5.320	0.663
0.900	0.190	3.177	0.502	6.034	0.708
1.374	0.262	3.925	0.551	6.714	0.737
		T = 45 °C			
0.399	0.046	2.122	0.265	4.776	0.419
0.666	0.092	2.735	0.310	5.422	0.462
1.000	0.138	3.381	0.354	6.136	0.489
1.238	0.164	4.061	0.392	6.714	0.519
1.612	0.214				
		T = 60 °C			
0.465	0.023	2.088	0.185	4.810	0.314
0.733	0.057	2.735	0.222	5.490	0.341
1.034	0.101	3.381	0.263	6.170	0.367
1.544	0.136	4.061	0.300	6.850	0.378

Table 2. Measured Equilibrium Amount Adsorbed (n) of Methane on Date-Pit Activated Carbon versus Increasing Pressure (P) from T = (30 to 60) °C

P atm	n mol·kg^{-1}	P atm	n mol·kg^{-1}	P atm	n mol·kg^{-1}
		T = 30 °C			
0.265	0.094	1.714	1.081	4.946	1.782
0.365	0.288	2.224	1.230	5.728	1.864
0.632	0.518	2.803	1.384	6.374	1.954
0.983	0.742	3.347	1.567	6.068	1.960
1.102	0.814	4.129	1.689	5.626	1.953
1.340	0.935				
		T = 45 °C			
0.232	0.106	2.054	0.932	4.946	1.422
0.432	0.263	2.701	1.082	5.728	1.501
0.733	0.461	3.449	1.204	6.476	1.576
1.000	0.623	4.163	1.327	6.170	1.567
1.510	0.770				
		T = 60 °C			
0.232	0.090	1.238	0.519	3.687	0.992
0.348	0.166	1.544	0.588	4.401	1.074
0.499	0.224	1.918	0.691	5.116	1.150
0.733	0.324	2.429	0.796	5.864	1.211
0.866	0.422	3.041	0.894	6.510	1.259
1.034	0.488				

were carbonized and activated to produce activated carbons. The carbonization was performed in a tube furnace which had been initially purged with a flow of nitrogen for 10 min. After that, the furnace was heated at a rate of 5 °C·min^{-1} up to 900 °C and was kept at that temperature for 3 h. After cooling down the furnace to room temperature, the material contained was considered as a carbonized (inactive carbon) adsorbent. Then, the carbonized adsorbent was activated in the same tube furnace and the same temperature program as in the carbonization step, but with a flow of carbon dioxide (instead of nitrogen). The resulting product is activated carbon.

The produced date-pit activated carbon was characterized at the UAE University laboratories with a Micromeritics ASAP 2010 instrument. The total surface area of the produced date-pit activated carbon was found to be 645 m^2·g^{-1}, of which 544 m^2·g^{-1} was in the micropore region. The corresponding total pore volume of date-pit activated carbon was found to be 0.287 cm^3·g^{-1}, of which 0.214 cm^3·g^{-1} was in the micropore region. Although the surface area obtained in this work is lower than conventional values for commercial activated carbons, the purpose of the current work is to explore the characteristics of activated carbons prepared from date pits to be used in the adsorption of various components. Nonetheless, an optimization of the carbonization and activation conditions is recommended to improve further the characteristics of the produced date-pit activated carbon.

Table 3. Measured Equilibrium Amount Adsorbed (n) of Ethane on Date-Pit Activated Carbon versus Increasing Pressure (P) from T = (30 to 60) °C

P atm	n mol·kg^{-1}	P atm	n mol·kg^{-1}	P atm	n mol·kg^{-1}
		T = 30 °C			
0.165	0.465	1.136	2.664	2.497	3.002
0.165	1.236	1.238	2.718	3.211	3.067
0.365	1.868	1.544	2.795	3.891	3.117
0.632	2.329	1.952	2.899	4.299	3.148
		T = 45 °C			
0.315	0.292	1.000	1.746	2.633	2.395
0.365	0.808	1.238	1.879	3.585	2.464
0.566	1.268	1.578	2.049	4.163	2.507
0.866	1.664	2.122	2.205	4.537	2.527
		T = 60 °C			
0.165	0.122	1.136	1.693	3.007	2.181
0.165	0.344	1.102	1.783	3.721	2.262
0.282	0.629	1.476	1.850	4.265	2.293
0.415	0.991	1.816	1.974	4.537	2.330
0.699	1.387	2.361	2.083		

High-purity nitrogen was obtained from the Sharjah Oxygen Company. High-purity methane (grade 3.5) was provided by Air Products. Ethane (99 % purity) and ethylene (99.5 % purity) were obtained from the Linde Gas Company Ltd. and Scott Specialty Gases, respectively. All gases were used as received from the supplier without any further purification.

The adsorption and desorption isotherm equilibria of nitrogen, methane, ethane, and ethylene were measured on date-pit activated carbon at three temperatures: (60, 45, and 30) °C. The adsorption and desorption measurements were performed systematically using the same apparatus and procedures described elsewhere.[18] The adsorption apparatus was hosted in a thermostatic oven which can be set in the temperature range of (30 to 220) °C with a precision of ± 1 °C.[18] The apparatus was tested to be leak-proof for pressures up to 110 psig. The pressure gauge was an analog type with a gauge pressure range of (−1 to 10) bar and an precision of 1 %,[18] whereas the vacuum pump had a vacuum rating of 20 μm Hg (20 mtorr).[18]

The measured adsorption data for nitrogen, methane, ethane, and ethylene are listed in Tables 1, 2, 3, and 4, respectively. Furthermore, the measured desorption data for nitrogen, methane, ethane, and ethylene are listed in Tables 5, 6, 7, and 8, respectively.

3. Theory

The dual-site Langmuir model (bimodal two-site discrete distribution with the Langmuir isotherm) provides a powerful framework to correlate gas adsorption equilibria because it has a flexible mathematical form for pure-gas adsorption.[19] In this work, a dual-site Langmuir model was adopted for correlating the adsorption equilibria, and it was modified to deal with desorption equilibria with hysteresis. The adsorption equilibria was described with a conventional dual-site Langmuir isotherm model, which is given by:

$$n_a = \sum_{i=1}^{2} \frac{m_i b_{i,a} P}{1 + b_{i,a} P} \quad (1)$$

where n_a is the amount adsorbed at pressure P, i (taking the value of 1 or 2) is the number of adsorption sites, and m_i and

Table 4. Measured Equilibrium Amount Adsorbed (n) of Ethylene on Date-Pit Activated Carbon versus Increasing Pressure (P) from T = (30 to 60) °C

P atm	n mol·kg^{-1}	P atm	n mol·kg^{-1}	P atm	n mol·kg^{-1}
		T = 30 °C			
0.232	0.759	1.544	2.494	3.993	2.986
0.432	1.468	2.020	2.674	4.367	3.006
0.833	2.074	2.735	2.818	4.265	3.043
1.000	2.154	3.449	2.929	4.503	3.072
1.170	2.317				
		T = 45 °C			
0.265	0.710	1.476	2.111	3.619	2.583
0.499	1.367	1.816	2.243	3.959	2.679
1.000	1.899	2.327	2.371	4.333	2.709
1.102	1.971	2.939	2.494	4.537	2.737
1.238	2.015				
		T = 60 °C			
0.181	0.117	1.068	1.621	3.551	2.265
0.198	0.333	1.204	1.668	3.993	2.333
0.232	0.541	1.408	1.775	4.333	2.368
0.465	0.985	1.782	1.900	4.537	2.394
0.733	1.385	2.259	2.038	4.571	2.445
1.000	1.542	2.837	2.176		

Table 5. Measured Equilibrium Amount Adsorbed (n) of Nitrogen on Date-Pit Activated Carbon versus Decreasing Pressure (P) from T = (30 to 60) °C

P atm	n mol·kg^{-1}	P atm	n mol·kg^{-1}	P atm	n mol·kg^{-1}
		T = 30 °C			
6.034	0.818	3.993	0.710	1.476	0.452
5.592	0.817	3.313	0.682	1.068	0.381
5.082	0.801	2.735	0.618	0.766	0.340
4.571	0.758	2.122	0.550		
		T = 45 °C			
6.306	0.507	3.891	0.438	1.408	0.212
5.762	0.497	3.313	0.393	1.000	0.155
5.218	0.467	2.701	0.343	0.699	0.126
4.571	0.450	2.088	0.283		
		T = 60 °C			
6.102	0.362	3.891	0.302	1.340	0.138
5.626	0.362	3.245	0.281	0.967	0.092
5.116	0.342	2.633	0.243	0.683	0.074
4.537	0.319	2.020	0.196		

$b_{i,a}$ are, respectively, the monolayer saturation limit and the adsorption affinity on the adsorption site i.

The dual-site Langmuir model is modified in this work to describe desorption data with hysteresis by adding a correction factor as shown in eq 2.

$$n_d = \sum_{i=1}^{2} \frac{m_i b_{i,d} P}{1 + b_{i,d} P} + \xi \tag{2}$$

where n_d is the amount remaining after desorption at pressure P, $b_{i,d}$ is the desorption affinity for the adsorption site i, and ξ is the correction factor added to the desorption equation to make it equal to the adsorption equation when reaching the maximum pressure (P_{max}) from which the desorption process starts. Equating eqs 1 and 2 at $P = P_{max}$ gives an expression for ξ, which can be substituted again into eq 2 to give:

$$n_d = \sum_{i=1}^{2} m_i \left[\frac{b_{i,d} P}{1 + b_{i,d} P} + \frac{(b_{i,a} - b_{i,d}) P_{max}}{(1 + b_{i,a} P_{max})(1 + b_{i,d} P_{max})} \right] \tag{3}$$

The adsorption and desorption affinities depend on temperature as shown by eqs 4 and 5, respectively:

$$b_{i,a} = b_{0i,a} \exp\left(\frac{\varepsilon_{i,a}}{RT}\right) \tag{4}$$

$$b_{i,d} = b_{0i,d} \exp\left(\frac{\varepsilon_{i,d}}{RT}\right) \tag{5}$$

where b_{0i} is a pre-exponential factor for the adsorption on site i, ε_i is the energy of adsorption or desorption of site i, R is the universal gas constant, and T is the absolute temperature.

The isosteric heat of adsorption is calculated through the Clausius−Clapeyron equation as:[3]

Table 6. Measured Equilibrium Amount Adsorbed (n) of Methane on Date-Pit Activated Carbon versus Decreasing Pressure (P) from T = (30 to 60) °C

P atm	n mol·kg^{-1}	P atm	n mol·kg^{-1}	P atm	n mol·kg^{-1}
		T = 30 °C			
5.116	1.932	3.313	1.808	1.748	1.451
4.571	1.894	2.803	1.721	1.408	1.314
3.857	1.862	2.293	1.606		
		T = 45 °C			
5.728	1.545	3.993	1.422	2.327	1.159
4.980	1.521	3.449	1.349	1.714	1.028
4.537	1.473	2.871	1.268	1.340	0.914
		T = 60 °C			
6.170	1.256	4.027	1.216	1.680	0.848
4.946	1.449	3.449	1.153	1.272	0.749
5.150	1.303	2.905	1.064	1.000	0.667
4.605	1.264	2.327	0.966	0.833	0.592

Table 7. Measured Equilibrium Amount Adsorbed (n) of Ethane on Date-Pit Activated Carbon versus Decreasing Pressure (P) from T = (30 to 60) °C

P atm	n mol·kg^{-1}	P atm	n mol·kg^{-1}	P atm	n mol·kg^{-1}
		T = 30 °C			
3.993	3.161	2.259	3.185	1.408	3.039
3.449	3.241	1.850	3.122	1.136	2.932
3.041	3.250	1.612	3.067	0.900	2.857
2.667	3.225				
		T = 45 °C			
4.265	2.533	2.395	2.431	1.544	2.245
3.891	2.531	1.952	2.362	1.170	2.156
3.449	2.503	1.680	2.305	1.000	2.057
2.905	2.473				
		T = 60 °C			
4.299	2.335	3.279	2.321	1.952	2.167
3.993	2.347	2.837	2.285	1.476	2.055
3.721	2.332	2.395	2.233	1.170	1.958

Table 8. Measured Equilibrium Amount Adsorbed (n) of Ethylene on Date-Pit Activated Carbon versus Decreasing Pressure (P) from T = (30 to 60) °C

P atm	n mol·kg^{-1}	P atm	n mol·kg^{-1}	P atm	n mol·kg^{-1}
		T = 30 °C			
4.265	3.072	3.041	3.040	2.088	2.912
3.891	3.069	2.735	3.014	1.782	2.842
3.313	3.056	2.361	2.972	1.408	2.710
		T = 45 °C			
4.333	2.741	2.769	2.627	1.544	2.359
3.993	2.728	2.327	2.563	1.238	2.243
3.585	2.715	1.952	2.482	1.000	2.151
3.177	2.682	1.714	2.413	0.866	2.067
		T = 60 °C			
4.367	2.439	2.735	2.205	1.374	1.835
3.993	2.422	2.224	2.111	1.102	1.743
3.517	2.391	1.952	2.016	0.983	1.638
3.313	2.264	1.680	1.961		

$$q_a = RT^2\left(\frac{\partial \ln P}{\partial T}\right)_{n_a} \quad (6)$$

When the isotherm is in the form of $n = n(P,T)$, eq 6 is changed to the following form by the chain rule of calculus:

$$q_a = \frac{-RT^2}{P}\left(\frac{\partial n_a}{\partial T}\right)_P \Big/ \left(\frac{\partial n_a}{\partial P}\right)_T \quad (7)$$

Applying eq 7 to eqs 1 and 4 results in the following expressions for the isosteric heat of adsorption

$$q_a = \frac{\sum_{i=1}^{2}\left(\frac{b_{i,a}m_i}{[1 + b_{i,a}P]^2}\varepsilon_{i,a}\right)}{\sum_{i=1}^{2}\left(\frac{b_{i,a}m_i}{[1 + b_{i,a}P]^2}\right)} \quad (8)$$

The isosteric heat of desorption can be defined similarly to eq 7.

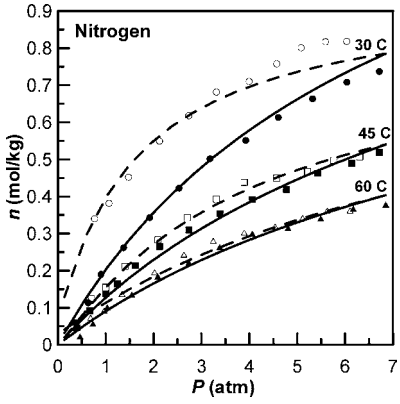

Figure 1. Experimental adsorption and desorption equilibrium data (solid and empty symbols, respectively) of nitrogen on date-pit activated carbon versus correlated adsorption and desorption data (solid and dashed lines, respectively).

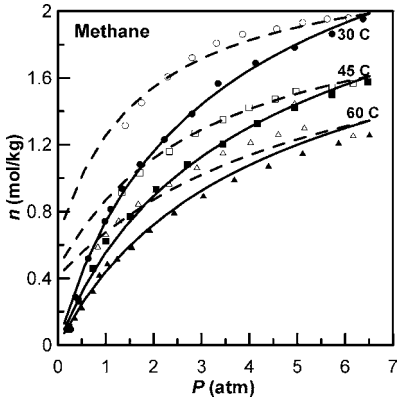

Figure 2. Experimental adsorption and desorption equilibrium data (solid and empty symbols, respectively) of methane on date-pit activated carbon versus correlated adsorption and desorption data (solid and dashed lines, respectively).

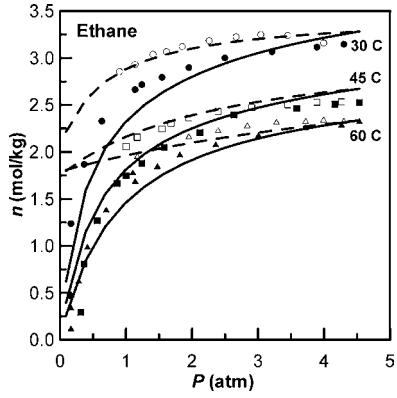

Figure 3. Experimental adsorption and desorption equilibrium data (solid and empty symbols, respectively) of ethane on date-pit activated carbon versus correlated adsorption and desorption data (solid and dashed lines, respectively).

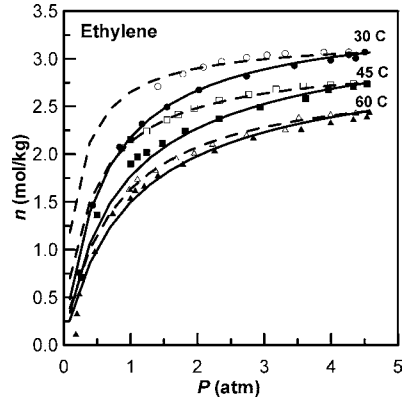

Figure 4. Experimental adsorption and desorption equilibrium data (solid and empty symbols, respectively) of ethylene on date-pit activated carbon versus correlated adsorption and desorption data (solid and dashed lines, respectively).

Table 9. Fitted Langmuir Adsorption and Desorption Isotherm Model Parameters and Average Relative Error (ARE)[a] Values

	nitrogen	methane	ethylene	ethane
m_1, mol·kg^{-1}	0.902	1.717	2.760	1.422
$10^6\ b_{01,a}$, atm^{-1}	3.26·10^{-06}	2349.343	3243.925	2.61·10^{-10}
$\varepsilon_{1,a}/R$, K	7269	1625	1948	10466
$10^6\ b_{01,d}$, atm^{-1}	0.002359	2.304919	10.82517	8.39·10^{-06}
$\varepsilon_{1,d}/R$, K	5863	3760	3881	7834
m_2, mol·kg^{-1}	0.777	1.472	0.724	2.698
$10^6\ b_{02,a}$, atm^{-1}	421.4086	0.000933	3.15·10^{-08}	62.31528
$\varepsilon_{2,a}/R$, K	1876	5683	9380	3275
$10^6\ b_{02,d}$, atm^{-1}	0	0	0	1.493086
$\varepsilon_{2,d}/R$, K	0	0	0	−2624
ARE_a, %	8.71	9.49	11.37	23.17
ARE_d, %	4.88	3.29	0.93	2.26
ARE, %	6.82	6.72	6.68	13.61

[a] ARE = overall average relative error; ARE_a = average relative error for adsorption data; ARE_d = average relative error for desorption data.

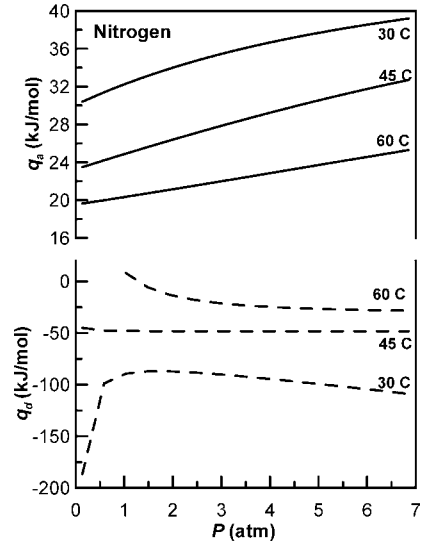

Figure 5. Isosteric heats of adsorption and desorption (solid and dashed lines, respectively) of nitrogen on date-pit activated carbon.

However, unlike adsorption (which is exothermic), desorption is an endothermic process. Therefore, it should have an opposite sign than eq 7. In other words, the isosteric heat of desorption is given by

$$q_{\mathrm{d}} = \frac{RT^2}{P}\left(\frac{\partial n_{\mathrm{d}}}{\partial T}\right)_P \Big/ \left(\frac{\partial n_{\mathrm{d}}}{\partial P}\right)_T \tag{9}$$

Applying eq 9 to eqs 3 through 5 results in the following expressions for the isosteric heat of desorption

$$q_{\mathrm{d}} = \frac{\sum_{i=1}^{2}\left(\left[\frac{b_{i,\mathrm{d}}m_i}{(1+b_{i,\mathrm{d}}P_{\max})^2}\left(\frac{P_{\max}}{P}\right) - \frac{b_{i,\mathrm{d}}m_i}{(1+b_{i,\mathrm{d}}P)^2}\right]\varepsilon_{i,\mathrm{d}} - \frac{b_{i,a}\varepsilon_{i,\mathrm{a}}m_i}{(1+b_{i,\mathrm{a}}P_{\max})^2}\left(\frac{P_{\max}}{P}\right)\right)}{\sum_{i=1}^{2}\left(\frac{b_{i,\mathrm{d}}m_i}{(1+b_{i,\mathrm{d}}P)^2}\right)} \tag{10}$$

4. Results and Discussion

The adsorption equilibria of nitrogen, methane, ethane, and ethylene measured on date-pit activated carbon are shown in Tables 1 through 4, respectively, and those of desorption equilibria are shown in Tables 5 through 8, respectively. Furthermore, the measured adsorption and desorption data are shown by the symbols in Figures 1, 2, 3, and 4 for nitrogen, methane, ethane, and ethylene, respectively. It should be noted that the estimation of these experimental data was based on nonideal gas pressure−volume−temperature calculations as described before.[18] This note has been shown to be important, especially when dealing with gases with relatively high molecular weights and at high pressures or low temperatures.

It is noted from Figures 1 through 4 that date-pit activated carbon exhibits hysteresis for the desorption of all gas species examined in this work. According to the IUPAC classification,[20] this hysteresis is considered to be of type H4. This type is often associated with narrow slit-like pores, but in this case the type I isotherm character is indicative of microporosity.[20]

This hysteresis phenomenon was most predominant at low temperatures (e.g., 30 °C), whereas it can sometimes be neglected at higher temperatures (e.g., 60 °C). Overall, the adsorption and desorption data for each component were fitted collectively (both adsorption and desorption, and at all temperatures simultaneously) using the Microsoft Excel's solver tool by varying the fitting parameters (i.e, m_1, $b_{01,\mathrm{a}}$, $\varepsilon_{1,\mathrm{a}}/R$, $b_{01,\mathrm{d}}$, $\varepsilon_{1,\mathrm{d}}/R$, m_2, $b_{02,\mathrm{a}}$, $\varepsilon_{2,\mathrm{a}}/R$, $b_{02,\mathrm{d}}$, and $\varepsilon_{2,\mathrm{d}}/R$) to minimize the following sum of squared errors (SSE):

$$\mathrm{SSE} = \sum_{j=1}^{N_{\mathrm{e,a}}}[n_{\mathrm{a,exp}} - n_{\mathrm{a,calc}}]_j^2 + \sum_{k=1}^{N_{\mathrm{e,d}}}[n_{\mathrm{d,exp}} - n_{\mathrm{d,calc}}]_k^2 \tag{11}$$

where $N_{\mathrm{e,a}}$ and $N_{\mathrm{e,d}}$ are the total number of experimental data points for adsorption and desorption, respectively, and n_{a} and n_{d} are the adsorbed amounts at the corresponding adsorption and desorption conditions, respectively. Subscripts "exp" and "calc" indicate experimental and correlated amounts, respectively; where the correlated amounts are calculated according to eqs 1, 3, 4, and 5. It should be noted that $P_{\max}$ values for nitrogen, methane, ethane, and ethylene were set at the overall maximum pressures of 6.85, 6.51, 4.54, and 4.57 atm, respectively.

Whenever possible, especially for the case of desorption isotherms, the second adsorption or desorption site parameters ($b_{02,\mathrm{a}}$, $\varepsilon_{2,\mathrm{a}}/R$, $b_{02,\mathrm{d}}$, and $\varepsilon_{2,\mathrm{d}}/R$) were excluded from the model by setting them to zero, as long as this did not affect the obtained minimum SSE. The resulting fitting parameters for nitrogen, methane, ethane, and ethylene on date-pit activated carbon are shown in Table 9 along with the corresponding average relative errors (AREs) for adsorption, desorption, and their combination (labeled as overall). The AREs have been calculated according to the following equation:

$$\mathrm{ARE}\ (\%) = \frac{100\ \%}{N_{\mathrm{e}}}\sum_{j=1}^{N_{\mathrm{e}}}\left[\frac{|n_{\mathrm{exp}} - n_{\mathrm{calc}}|}{n_{\mathrm{exp}}}\right]_j \tag{12}$$

where N_{e} is the corresponding number of experimental data points. The resulting adsorption and desorption isotherm correlations were also plotted versus the experimental data for nitrogen, methane, ethane, and ethylene as shown by the lines in Figures 1 through 4, respectively.

Table 9 shows that the overall ARE values of nitrogen, methane, and ethylene are all less than 10 %. The overall ARE of ethane is slightly above 10 %, but this could be due to combined sources of errors (such as combinations of both experimental and correlation errors) and not purely a correlation error. Furthermore, the ARE values of correlating the desorption equilibria of all of the components were in the range of (0.93 to 4.88) %. Therefore, the proposed Langmuir type model is considered very satisfactory for fitting such adsorption−desorption equilibria which exhibit temperature-dependent hysteresis phenomena. It can also be noted that the fitting parameters corresponding to the first adsorption site (i.e., m_1, $b_{01,\mathrm{a}}$, $\varepsilon_{1,\mathrm{a}}/R$, $b_{01,\mathrm{d}}$, $\varepsilon_{1,\mathrm{d}}/R$) are more significant than those of the second adsorption site. Thus, it is suggested that date-pit activated carbon can sufficiently be described with a patch-wise heterogeneous adsorption surface. In several cases, the second-site desorption parameters were successfully set to zero without affecting the obtained minimum SSE as shown in Table 9.

The isosteric heats of adsorption and desorption are calculated from the fitted adsorption and desorption isotherms using eqs 8 and 10, respectively. The resulting isosteric heats of adsorption and desorption of nitrogen, methane, ethane, and ethylene are shown in Figures 5, 6, 7, and 8, respectively, where positive heat values indicate exothermic adsorption processes and negative heat values indicate endothermic desorption processes.

Figures 5 through 8 show that the isosteric heats of adsorption usually increase with pressure and hence with surface coverage. This indicates that the adsorption of these components on date-pit activated carbon is characterized with favorable lateral interactions of the adsorbed molecules on a relatively homogeneous surface of the adsorbent.[21] This observation is consistent with the former observation of the insignificant contribution of the second adsorption site as indicated above.

It is also noted that the isosteric heats of adsorption (solid lines in Figures 5 through 8) increase with temperature for all of the components, except for ethylene where the heats of adsorption become independent of temperature at a pressure of ~ 3.2 atm and in the temperature range of (30 to 45) °C. In general, the adsorption of such components is most exothermic

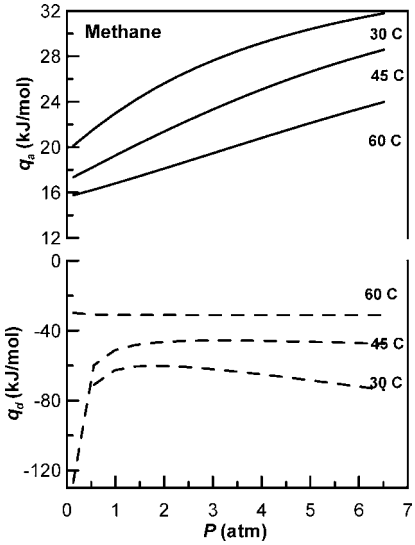

Figure 6. Isosteric heats of adsorption and desorption (solid and dashed lines, respectively) of methane on date-pit activated carbon.

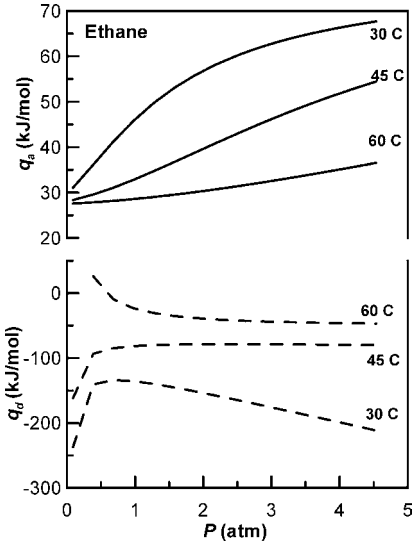

Figure 7. Isosteric heats of adsorption and desorption (solid and dashed lines, respectively) of ethane on date-pit activated carbon.

at low temperatures (e.g., at 30 °C), especially for heavy components such as ethane. On the other hand, the isosteric heats of desorption are also most endothermic at low temperatures (e.g., at 30 °C) at either very low or very high pressures. Nonetheless, the absolute value of the isosteric heat of desorption of various components is much greater than that of adsorption. This is consistent with the hysteresis effect where the adsorbed molecules do not favor transferring to the gas phase unless they are provided with high energies to counteract their attraction forces to the surface of the adsorbent. This phenomenon also indicates that having an adsorption−desorption cycle (by cycling pressures between low and high values) on an adsorbent that exhibits a hysteresis phenomenon (such as a date-pit activated carbon) results in a net endothermic heat effect. Such observations may become a useful seed to make a cooling process on the basis of pressure swinging (adsorption and desorption) of specific gas compounds on such adsorbent surfaces.

5. Conclusions

An agricultural byproduct (i.e., date pits) was chosen as a candidate of adsorbent material for vapor phase adsorption. Date pits were harvested, dried, screened, carbonized, and activated to produce a highly porous activated carbon. The adsorption and desorption isotherms of nitrogen, methane, ethane, and ethylene were measured on the produced date-pit activated carbon using a volumetric adsorption apparatus and nonideal gas correlations. It was observed that the measured adsorption and desorption equilibria exhibit a hysteresis phenomenon, especially at lower temperatures. The adsorption−desorption equilibria were fitted successfully with a modified temperature-dependent, dual-site Langmuir isotherm model. Furthermore, it was observed that desorption requires more energy than that of the adsorption of the same compound at the same conditions, especially at low temperatures and high pressures.

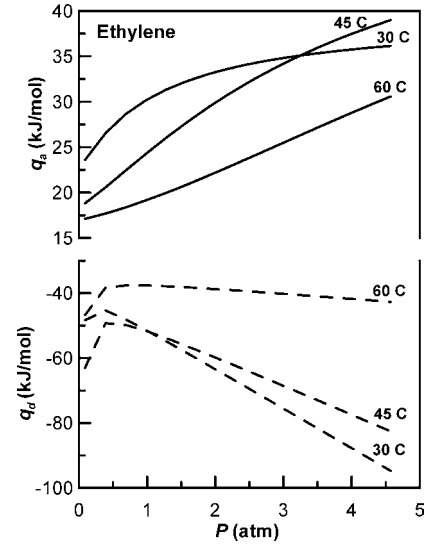

Figure 8. Isosteric heats of adsorption and desorption (solid and dashed lines, respectively) of ethylene on date-pit activated carbon.

Acknowledgment

The laboratory technicians H. Kamal, S. Al-Hardelo, and M. Hussein helped to conduct the experimental work reported in this project. The Department of Chemical and Petroleum Engineering at the United Arab Emirates University was very helpful and put every effort to facilitate the experimental work towards its successful completion.

Literature Cited

(1) Yang, R. T. *Gas Separation by Adsorption Processes*; Imperial College Press: London, 1997.
(2) Ruthven, D. M. *Principles of Adsorption and Adsorption Processes*; John Wiley and Sons: New York, 1984.
(3) Valenzuela, D. P.; Myers, A. L. *Adsorption Equilibrium Data Handbook*; Prentice-Hall, Inc.: Upper Saddle River, NJ, 1989.
(4) Banat, F.; Al-Asheh, S.; Al-Makhadmeh, L. Evaluation of the use of raw and activated date pits as potential adsorbents for dye containing waters. *Process Biochem. (Oxford, U.K.)* **2003**, *39*, 193–202.
(5) Banat, F.; Al-Asheh, S.; Al-Makhadmeh, L. Utilization of Raw and Activated Date Pits for the Removal of Phenol from Aqueous Solutions. *Chem. Eng. Technol.* **2004**, *27*, 80–86.
(6) El-Hendawy, A. A. The role of surface chemistry and solution pH on the removal of Pb^{2+} and Cd^{2+} ions via effective adsorbents from low-cost biomass. *J. Hazard. Mater.* **2009**, *167*, 260−267.
(7) El-Sharkawy, E. A.; Soliman, A. Y.; Al-Amer, K. M. Comparative study for the removal of methylene blue via adsorption and photocatalytic degradation. *J. Colloid Interface Sci.* **2007**, *310*, 498–508.
(8) Al-Muhtaseb, S. A.; El-Naas, M. H.; Abdallah, S. Removal of Aluminum from Aqueous Solutions by Adsorption on Date-Pit and BDH Activated Carbons. *J. Hazard. Mater.* **2008**, *158*, 300–307.
(9) Saad, E. M.; Mansour, R. A.; El-Asmy, A.; El-Shahawi, M. S. Sorption profile and chromatographic separation of uranium (VI) ions from aqueous solutions onto date pits solid sorbent. *Talanta* **2008**, *76*, 1041–1046.

(10) Tovbin, Y. K. Condition for an adsorption hysteresis loop to appear in narrow cylindrical pores. *Russ. Chem. Bull.* **2004**, *53*, 2884–2885.
(11) Ball, P. C.; Evans, R. On the Mechanism for Hysteresis of Gas Adsorption on Mesoporous Substrates. *Europhys. Lett.* **1987**, *4*, 715–721.
(12) Liu, J. C.; Monson, P. A. Monte Carlo simulation study of water adsorption in activated carbon. *Ind. Eng. Chem. Res.* **2006**, *45*, 5649–5656.
(13) Jorge, M.; Schumacher, C.; Seaton, N. A. Simulation study of the effect of the chemical heterogeneity of activated carbon on water adsorption. *Langmuir* **2002**, *18*, 9296–9306.
(14) McCallum, C. L.; Bandosz, T. J.; McGrother, S. C.; Muller, E. A.; Gubbins, K. E. A molecular model for adsorption of water on activated carbon: Comparison of simulation and experiment. *Langmuir* **1999**, *15*, 533–544.
(15) Muller, E. A.; Rull, L. F.; Vega, L. F.; Gubbins, K. E. Adsorption of water on activated carbons: A molecular simulation study. *J. Phys. Chem.* **1996**, *100*, 1189–1196.
(16) Wongkoblap, A.; Do, D. D. The effects of curvature and surface heterogeneity on the adsorption of water in finite length carbon nanopores: A computer simulation study. *Mol. Phys.* **2008**, *106*, 627–641.
(17) Do, D. D.; Junpirom, S.; Do, H. D. A New Adsorption-Desorption Model for Water Adsorption in Activated Carbon. *Carbon* **2009**, *47*, 1466−1473.
(18) Al-Muhtaseb, S. A.; Abu Al-Rub, F. A.; Al Zarooni, M. Adsorption Equilibria of Nitrogen, Methane and Ethane on BDH Activated Carbon. *J. Chem. Eng. Data* **2007**, *52*, 60–65.
(19) Mathias, P. M.; Kumar, R.; Moyer, J. D., Jr.; Schork, J. M.; Srinivasan, S. R.; Auvil, S. R.; Talu, O. Correlation of Multicomponent Gas Adsorption by the Dual-Site Langmuir Model. Application to Nitrogen/Oxygen Adsorption on 5A-Zeolite. *Ind. Eng. Chem. Res.* **1996**, *35*, 2477–2483.
(20) Sing, K. S. W.; Everett, D. H.; Haul, R. A. W.; Moscou, L.; Pierotti, R. A.; Rouquerol, J.; Siemieniewska, T. Reporting Physisorption Data for Gas/Solid Systems with Special Reference to the Determination of Surface Area and Porosity. *Pure Appl. Chem.* **1985**, *57*, 603–619.
(21) Al-Muhtaseb, S. A.; Ritter, J. A. Roles of Surface Heterogeneity and Lateral Interactions on the Isosteric Heat of Adsorption and Adsorbed Phase Heat Capacity. *J. Phys. Chem. B* **1999**, *103*, 2467–2479.

Received for review April 13, 2009. Accepted October 2, 2009. The author appreciates the financial support from Research Affairs at the United Arab Emirates University under grants # 04-02-7-11/05 and 01-03-02-7-11/07.

JE900350K